Biology of Reproduction, 2023, **109(3)**, 340–355
https://doi.org/10.1093/biolre/ioad069
Advance access publication date 3 July 2023
Research Article

ADAD1 is required for normal translation of nuclear pore and transport protein transcripts in spermatids of *Mus musculus*†

Sarah Potgieter[1], Christopher Eddy[1], Aditi Badrinath[1], Lauren Chukrallah[1], Toby Lo[1], Gayatri Mohanty[2], Pablo E. Visconti[2] and Elizabeth M. Snyder[1,*]

[1]Department of Animal Sciences, Rutgers, The State University of New Jersey, New Brunswick, NJ, USA
[2]Department of Veterinary and Animal Sciences, University of Massachusetts, Amherst, MA, USA

***Correspondence:** Department of Animal Sciences, Rutgers, The State University of New Jersey, Foran Hall 328, 59 Dudley Rd, New Brunswick, NJ 08901, USA. E-mail: elizabeth.snyder@rutgers.edu

†**Grant Support:** Eunice Kennedy Shriver National Institute of Child Health and Human Development (NIH-NICHD F32 HD072628, K99/R00 HD083521, and R03 HD108418 to ES along with HD038082 and HD088571 to PV) and Rutgers University (to ES).

Abstract

ADAD1 is a testis-specific RNA-binding protein expressed in post-meiotic spermatids whose loss leads to defective sperm and male infertility. However, the drivers of the *Adad1* phenotype remain unclear. Morphological and functional analysis of *Adad1* mutant sperm showed defective DNA compaction, abnormal head shaping, and reduced motility. Mutant testes demonstrated minimal transcriptome changes; however, ribosome association of many transcripts was reduced, suggesting ADAD1 may be required for their translational activation. Further, immunofluorescence of proteins encoded by select transcripts showed delayed protein accumulation. Additional analyses demonstrated impaired subcellular localization of multiple proteins, suggesting protein transport is also abnormal in *Adad1* mutants. To clarify the mechanism giving rise to this, the manchette, a protein transport microtubule network, and the LINC (linker of nucleoskeleton and cytoskeleton) complex, which connects the manchette to the nuclear lamin, were assessed across spermatid development. Proteins of both displayed delayed translation and/or localization in mutant spermatids implicating ADAD1 in their regulation, even in the absence of altered ribosome association. Finally, ADAD1's impact on the NPC (nuclear pore complex), a regulator of both the manchette and the LINC complex, was examined. Reduced ribosome association of NPC encoding transcripts and reduced NPC protein abundance along with abnormal localization in *Adad1* mutants confirmed ADAD1's impact on translation is required for a NPC in post-meiotic germ cells. Together, these studies lead to a model whereby ADAD1's influence on nuclear transport leads to deregulation of the LINC complex and the manchette, ultimately generating the range of physiological defects observed in the *Adad1* phenotype.

Summary Sentence:
ADAD1 is a post-meiotic spermatid RNA-binding protein that is required for normal translation of mRNAs important for post-meiotic differentiation and mRNAs associated with nuclear and intracellular transport.

Graphical Abstract

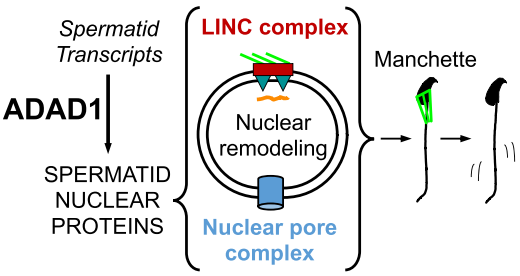

Keywords: spermiogenesis, spermatids, RNA-binding proteins, translation regulation, manchette, LINC complex, microtubules, protein transport, nuclear pore complex

Introduction

Male fertility relies on the proper progression of male germ-cell differentiation, which has three phases: mitosis, meiosis, and finally spermiogenesis that generates the complex morphology of normal sperm. As such, spermiogenesis requires coordination of multiple events including DNA or genome compaction, head reshaping, tail building, and acrosome formation [1]. Although giving rise to distinct

Received: November 28, 2022. **Revised:** March 23, 2023. **Accepted:** June 29, 2023.

outcomes, many of the proteins and regulatory mechanisms are shared by one or more of these processes, leading to their overall interdependence [2]. Failure of one or more of these events leads to subfertility or sterility. As such, understanding their regulation is fundamental to defining underlying causes of male infertility.

One essential regulatory mechanism throughout spermiogenesis occurs on the level of translation and often impacts mRNA storage or translation itself [3]. While transcription is the first level of regulation in most cellular processes, male germ cells undergo post-meiotic genome compaction; thus, cells progress from a state of high transcription to nearly silent transcription during their differentiation. Translational regulation allows post-meiotic germ cells to resolve the disconnect between ongoing cellular processes and a lack of transcription as many spermiogenesis mRNAs are generated early (as early as late meiosis) and stored until translated [4]. This translation regulation leverages a wide range of RNA-binding proteins, not all of which have been fully described or identified. Also, while translation regulation has been implicated as regulating diverse aspects of genome compaction and tail building, how it regulates other important spermiogenesis events is less clear.

Perhaps the best described examples of translationally regulated spermiogenesis mRNAs encode the major genome compaction proteins, transition proteins 1 and 2 (TNP1 and 2) and protamine 1 and 2 (PRM1 and 2), which are expressed starting late in meiosis and undergo translation suppression until activation during mid- to late spermiogenesis [5–8]. Mutations that impact translation of these proteins are associated with severe differentiation defects. For example, mice with *Prm1* 3′ UTR loss exhibit no translation repression and have early DNA compaction with a total arrest of spermatid differentiation [9]. In addition, mice with a mutation in a protein involved in regulating translation of PRM1, protamine1 RNA-binding protein (PRBP), are oligozoospermic and infertile [10].

In addition to effective translation control, correct protein localization is fundamental for proper genome compaction. Upon cytoplasmic accumulation of the encoded proteins, they are imported into the nucleus to drive genome compaction as well as dramatic reduction in nuclear volume to facilitate packaging into the sperm head [11, 12]. However, it is unclear how translation and nuclear import are coordinated during spermiogenesis. It is known that abnormal localization of PRM1 and TNP1 is correlated with defective chromatin structure and reduced motility [13, 14]. In addition, it has been demonstrated that the localization of human growth hormone (hGH) fused to the 3′ UTR of *Prm1* is dependent on the timing of its translation [15], suggesting that the two events are linked. The mechanism driving this link is entirely unexplored.

In post-meiotic germ cells, translation regulation is mediated by RNA-binding proteins (RBPs) and their loss can lead to dramatic cellular defects [16–18]. In spite of advances in our understanding of RBP influence on translation during spermiogenesis, it is probable that many post-meiotic translation regulators remain undiscovered. Adenosine deaminase domain containing 1 (ADAD1), previously known as TENR, is a testis-specific RNA-binding protein expressed predominantly in post-meiotic round spermatids [19, 20]. Mice mutant for *Adad1* show infertility, severe sperm morphology defects, and high numbers of testis-retained spermatids [20]. Although ADAD1's molecular function is yet to be detailed, early analyses showed ADAD1 binds to reproductively important mRNAs such as *Prm1*. As such, ADAD1 was initially proposed as a putative translation regulator in spermatids [19]. Later work, however, suggested ADAD1 may act as an RNA editing enzyme given the presence of a double-stranded RNA-binding motif along with an adenosine deaminase (AD) domain [21], protein domains observed in other RNA editing enzymes [22]. Most recently, it was shown ADAD1's AD domain appears to be catalytically inactive and mutation of *Adad1* does not impact RNA editing of testicular mRNAs [20]. These disparate observations leave the true molecular function of ADAD1 unknown.

To identify the molecular function and downstream impacts of ADAD1 during spermiogenesis, we better defined morphology defects in *Adad1* mutant sperm. Based on these observations, we asked whether ADAD1 impacts the translation of transcripts associated with the observed morphological defects. In addition to showing delayed translation of several spermiogenesis regulating mRNAs, these analyses also showed an abnormal localization pattern of impacted proteins in *Adad1* mutants. Further molecular analyses demonstrated significant abnormalities in spermatid microtubules and the complex connecting the cytoplasmic microtubule network to the nucleus. We additionally determined that the nuclear pore complex requires ADAD1 for its normal translation. Ultimately, these studies reveal ADAD1 as a potent regulator of spermiogenesis, possibly via translation regulation.

Materials and methods

Animal model generation and husbandry

All protocols related to animal care and husbandry were approved and in accordance with guidelines from the Rutgers Institutional Animal Care and Use Committee and within AALAC and IACUC guidelines. *Adad1*$^{KO/KO}$ mice were generated as described in [20]. RiboTag mice [23] were purchased from The Jackson Laboratory and the *Adad1-RiboTag* mice were generated as described in [24] with *Adad1* as the gene of interest. The mice were housed in climate-controlled, sterile conditions with consistent 12-h light–dark cycles. Mice were fed with irradiated rodent chow (LabDiet 5058) and had ad libitum access to food and water.

Microscope imaging

A custom-built Zeiss microscope with both brightfield and fluorescent capabilities was used for all imaging. MetaMorph imaging software (Molecular Devices) was used for imaging of each channel individually, and channels were color-combined using the program's internal color combine tool. All images are representative of biological triplicate or greater. All quantification was done via direct visualization.

Epididymal sperm staining and functional analyses

See Supplemental Methods.

Testicular cell spreads and ICC

Testicular cell spreads were prepared based on a protocol described in [25]. In brief, triplicate wildtype and *Adad1*$^{KO/KO}$ 119 dpp testes were collected in 1× PBS and added to a DNase I/Collagenase I solution, which was then placed in a rotator at 37°C for 10 min. Tubules were left to settle for 2 min at room temperature and the somatic cell containing supernatant removed. Further digestion of the tubules was achieved by adding a DNase I/Collagenase I/Trypsin solution and rotating for 25 min at 37°C. The resulting cell solution

was sequentially passed through a 100 and 40 μm nylon strainer. Cells were then fixed in 4% PFA with 4% sucrose for 15 min at room temperature, washed in 1× PBS, and resuspended in 5 mL of 1× PBS with 0.05% Tween. Cell suspension (50 μL) was applied to uncharged slides and left at room temperature to air dry.

Before staining, slides were permeabilized with 1% Triton in 1× PBS at 37°C for 5 min, washed with 0.05% Tween in PBS, and blocked with 10% normal goat serum for 1 h at room temperature. Primary antibody was appropriately diluted in 10% goat serum and slides were incubated in a humid chamber overnight at 4°C. The next day, slides were washed with 0.05% Tween in PBS and fluorescent secondary antibody diluted in 0.05% Tween 1× PBS was added to slides for incubation in a light-protected humid chamber for 1 h at room temperature. Slides were then washed twice with 0.05% Tween in 1× PBS for 5 min and then once with 1× PBS for 5 min. Finally, slides were then mounted with DAPI Fluoromount-G (SouthernBiotech) and visualized on a microscope as stated above.

Immunofluorescence

Wildtype and *Adad1*$^{KO/KO}$ 60–70 dpp testes were collected from mice and fixed in 4% PFA overnight. Tissue was rinsed with PBS, dehydrated in ethanol, embedded in paraffin wax, and cut into 4 μm sections. Slides were deparaffinized in xylene, rehydrated, and antigen retrieval was done by boiling slides in Tris–EDTA (10 mM Tris–HCl, 1 mM EDTA, 0.05% Tween: pH 9.0) for 30 min. Slides were blocked with 3% goat serum and primary antibodies were applied and slides incubated overnight at room temperature. Slides were washed the next day in 0.1% Triton X-100, and fluorescence secondary antibody was added for a 1 h incubation with light protection. Slides were then mounted with DAPI Fluoromount-G (SouthernBiotech) and visualized as above. For a detailed description of antibody conditions, see Supplementary Table S1. For all quantification, a biological replicate of $n = 3$ was used. Forty tubules per stage were categorized based on staining pattern, except for stage XII, of which as many as possible were categorized. The stage of seminiferous tubule sections was determined according to the criteria described in [26], as well as using SYCP3 and DAPI staining. Since *Adad1*$^{KO/KO}$ have abnormal spermatid morphology as well as testis-retained spermatids, staging was mostly reliant on SYCP3 staining in spermatocytes and DAPI staining in spermatogonia.

Hematoxylin and eosin staining

Wildtype and *Adad1*$^{KO/KO}$ 25 dpp testes were collected and fixed in Bouin's Solution (Sigma Aldrich) overnight. Testis tissue was cleared in deionized water and dehydrated in increasing ethanol concentrations before dehydration, xylene clearing, embedding in paraffin, and cutting into 4 μm sections. Slides were deparaffinized in xylene, rehydrated in decreasing ethanol concentrations, and stained with Harris hematoxylin (Sigma Aldrich). Slides were rinsed in water, partially dehydrated in ethanol, and then stained with Eosin Y (Sigma Aldrich). Slides were then fully dehydrated and mounted with Permount mounting medium (Fisher Scientific) for visualization as above. Round spermatids were counted as detailed by [26] and were reported as the average number of round spermatids per tubule by biological replicate. At least 50 tubules were counted per biological sample ($n = 3$).

RiboTag RNA immunoprecipitation

Testes were collected from 28 dpp wildtype or *Adad1*$^{KO/KO}$ heterozygous for *Rpl22-HA* and *Stra8-iCre* [23, 24] ($n = 3$/genotype). This timepoint was selected to enrich for round spermatids transcripts [27]. The full immunoprecipitation and RNA extraction was conducted as in [24]. In brief, both wildtype and mutant testes were homogenized in lysis buffer and precleared with antibody-free magnetic beads before an input sample was collected. The lysate was incubated with anti-HA antibody (ABCAM) overnight, then precipitated with Protein A Dynabeads (Invitrogen). Beads were washed and RNA extracted using the miRNeasy mini kit (Qiagen). From each biological replicate, paired input and immunoprecipitated (IP) RNA samples were collected and pairing information retained for downstream analyses.

RNA sequencing

Input and IP RNA was quantified and sent to Genewiz (South Plainfield, NJ) for commercial sequencing (Total RNA, Illumina HiSeq 4000, paired-end, 150 bp reads). Strand-specific libraries were prepped with the Ribo-zero Gold HMR and TruSeq Stranded Total RNA Library Prep Human/Mouse/Rat. Quality control was tested using the FastQC software (Babraham Bioinformatics). FastQC reads were summarized with MultiQC (version 1.9) [28]. BOWTIE2 (version 2.4.1) [29] was used for in silico rRNA removal. Based on FastQC read results, the first 10 base pairs and last 20 base pairs were trimmed using TRIMMOMATIC [30] yielding 120 bp, paired-end reads. A rerun of FastQC and MultiQC showed improved quality of RNA samples. Confirmation of sample assignment was done using pcaExplorer [31] for principal component analysis. All RNA-seq data for this manuscript are available at https://www.ncbi.nlm.nih.gov/sra under accession PRJNA907786.

Bioinformatic data analysis

A novel testis-specific transcriptome [32] was appended to the Ensembl mouse transcriptome (Mus_musculus.GRCm38.90, mm10) to generate the expanded transcriptome used for analysis. Alignment was done with RSEM (version 1.3.3) [33] and fold change and differential expression calculated with EBSEQ (release 3.12) [34]. A cutoff of PPDE ≥ 0.95 was set to get a list of differentially expressed (DE) genes. Wildtype versus mutant fold change (FC) of greater than or less than one defined lists of depleted in mutant and enriched in the mutant, respectively. In addition, FC > 2 and FC < 0.5 were assigned for transcripts high depleted or enriched. Ribosome association (RA) was calculated by taking the ratio of the IP TPM to the input TPM. To avoid any division errors, transcripts were only calculated if input values were greater than 0. A Welch *t*-test was conducted using an R package matrixTests (version 0.1.9) [35] to identify differentially ribosome-associated transcripts (DRA, $P < 0.05$). Graphical visualization of data was largely done in RStudio (R Core Team, 2021). Scatterplots and heatmaps were done in base R. Cell-type-specific gene expression heatmaps were generated from data in publicly available datasets as described in [20]. Ontology analysis was conducted using DAVID Bioinformatics Resource (version 6.8) [36]. Differentially expressed or ribosome associated in wildtype or *Adad1*$^{KO/KO}$ samples were clustered with medium stringency by DAVID and categories with P values <0.05 were selected as significant.

Results

Loss of ADAD1 leads to abnormal sperm head morphology and motility

Adad1 mutants have previously been described as having reduced sperm production and severely defective morphology [21]. To better identify the aspects of spermiogenesis on which *Adad1* may be acting, we undertook a detailed analysis of *Adad1* mutant caudal sperm. First, DNA compaction was examined via aniline blue staining, which stains lysine-rich proteins such as histones but not protamines, which are rich with arginine and cysteine [37]. As such, aniline blue is an indirect measure of DNA compaction by acting as a proxy for the histone to protamine exchange that occurs during mid- and late spermiogenesis. This analysis (Supplementary Figure S1A and B) showed an 8.5-fold increase in the frequency of cells with strong aniline blue staining in *Adad1* mutants as compared to wildtype, demonstrating increased histone retention in mutant sperm and suggesting genome compaction may be defective in *Adad1* mutant sperm.

As a more direct measure of DNA compaction, we stained epididymal sperm with the DNA-staining dye DAPI and quantified areas of intense DAPI staining, which correlates with highly compact DNA [38, 39] (Supplementary Figure S1C and D). This analysis showed that mutant sperm had a general reduction in regions of intense DAPI staining in agreement with the increase in aniline blue staining and suggesting an overall reduction in DNA compaction. Previous reports have suggested that DAPI and protamines bind DNA competitively [40], thus potentially confounding our analysis. To eliminate this possibility, we utilized a secondary fluorescent DNA stain, chromomycin A3 (CMA3) [41]. Comparison of CMA3 and DAPI staining (Supplementary Figure S1E) demonstrated near perfect complementarity in CMA3-positive cells, confirming the effectiveness of using DAPI intensity to quantify DNA compaction. Thus, we quantified intense DAPI staining as a function of head volume. In mutant sperm, this analysis showed (1) an overall reduction in head volume (Supplementary Figure S1G) and (2) a reduced fraction of the head volume is composed of intense DAPI staining (Supplementary Figure S1H). Together, these results suggest a defect in DNA compaction in *Adad1* mutant sperm and further show a potentially broader abnormality leading to overall head morphology defects.

Findings from a previous genetic model suggested that mutation of *Adad1* leads to defective sperm motility [21]. To determine if this was the case in our model, we performed computer-aided sperm analysis on capacitated wildtype and mutant caudal sperm (Supplementary Figure S2A and B). This analysis revealed a distinct reduction in motility. In particular, progressive motility and hyperactivation were significantly reduced in the mutant versus the wildtype. To determine what may be driving this reduction, we examined activation of the protein kinase A(PKA) pathway, which is required for normal sperm motility [42], by quantifying PKA autophosphorylation as well as downstream tyrosine phosphorylation (Supplementary Figure S2C–F). Mutants showed significant reduction in both cases, suggesting that PKA activation is impaired in mutant sperm.

Adad1 mutant testes display limited changes in transcript abundance

Our morphological and functional analyses indicate that ADAD1 may be upstream of multiple spermiogenesis processes. To determine the mechanism by which ADAD1 may influence them, we examined total transcript abundance in 28 dpp whole testis. Subtle changes in transcript abundance may not be detected using this paradigm due to dilution from other testicular cell types. However, ADAD1 is predominantly expressed in round spermatids [20, 21] and this time point was selected to allow robust detection of round spermatid transcripts, which dominate the testis transcriptome at this time [27]. This point further reduces the frequency of elongating spermatids, a cell population likely to be disproportionally impacted by indirect ADAD1 effects. This analysis identified very few changes in transcript abundance (Figure 1A). Using an expanded testis transcriptome [32], over 55,000 genes were detected; however, only 245 (0.43% of total detected transcripts) were determined to be significantly differentially expressed (DE) between wildtype and *Adad1* mutant testes (Supplementary Table S2). Of these, only 78 (0.14% of total detected transcripts) were up- or downregulated by 2-fold or more in the mutant. Based on ontological and gene-level analyses (see Supplemental Results, Supplementary Table S3, and Supplementary Figure S1I and J for a full description), no cohesive changes in gene expression could be identified that would lead to the *Adad1* mutant phenotype.

Loss of ADAD1 leads to reduced ribosome association of spermatid transcripts

Overall, the above analyses demonstrated that the molecular action of ADAD1 is likely downstream of transcription, but upstream of multiple spermiogenesis controlling pathways. As ADAD1 was initially identified as a protein that bound the 3′ UTR of spermiogenesis-important transcripts [19], we next asked whether *Adad1* mutant testes had any observable translation defects by leveraging the transgenic RiboTag model [23]. In this model, an HA-tagged large ribosomal subunit protein is expressed under a cell-specific Cre driver [24], which allows cell-type-specific ribosome labeling. Labeled ribosomes can then be used to isolate ribosome-associated mRNAs via immunoprecipitation (IP). To determine transcriptome-wide changes in ribosome-associated mRNAs with ADAD1 loss, we generated wildtype and *Adad1* mutant mice in which *Stra8-iCre* drove RiboTag expression specifically in differentiating germ cells. RNA sequencing of HA immunoprecipitated (IP) samples from 28 dpp testes was then used to quantify ribosome association (RA) as a function of genotype. To correct for any ADAD1-dependent differences in transcript abundance, RA was expressed as the ratio of IP over total RNA and significant differential ribosome association (DRA) was then determined (Figure 1C). Based on morphological analyses, DRA did not appear to be driven by changes in tissue cellularity (Supplementary Figure S1I and J). We identified 1211 transcripts (4.41% of the total detected) with differential ribosome association between wildtype and *Adad1* mutant testes. The majority (1070 or 88.4% of DRA transcripts) had lower ribosome association in mutants (Supplementary Table S4) relative to wildtype. Ontological analysis of DRA transcripts showed enrichment of multiple categories important for spermiogenesis, the most significant of which were spermatogenesis, protein transport, microtubule cytoskeleton organization, mitotic cell cycle, microtubule-based process, and cell differentiation. These categories included genes that may be causative to the morphological defects previously identified. Among these were transition protein 1 (*Tnp1*), protamine 1 and 2 (*Prm1*, *Prm2*), and A-kinase anchoring protein 4 (*Akap4*), all of which showed significantly reduced ribosome

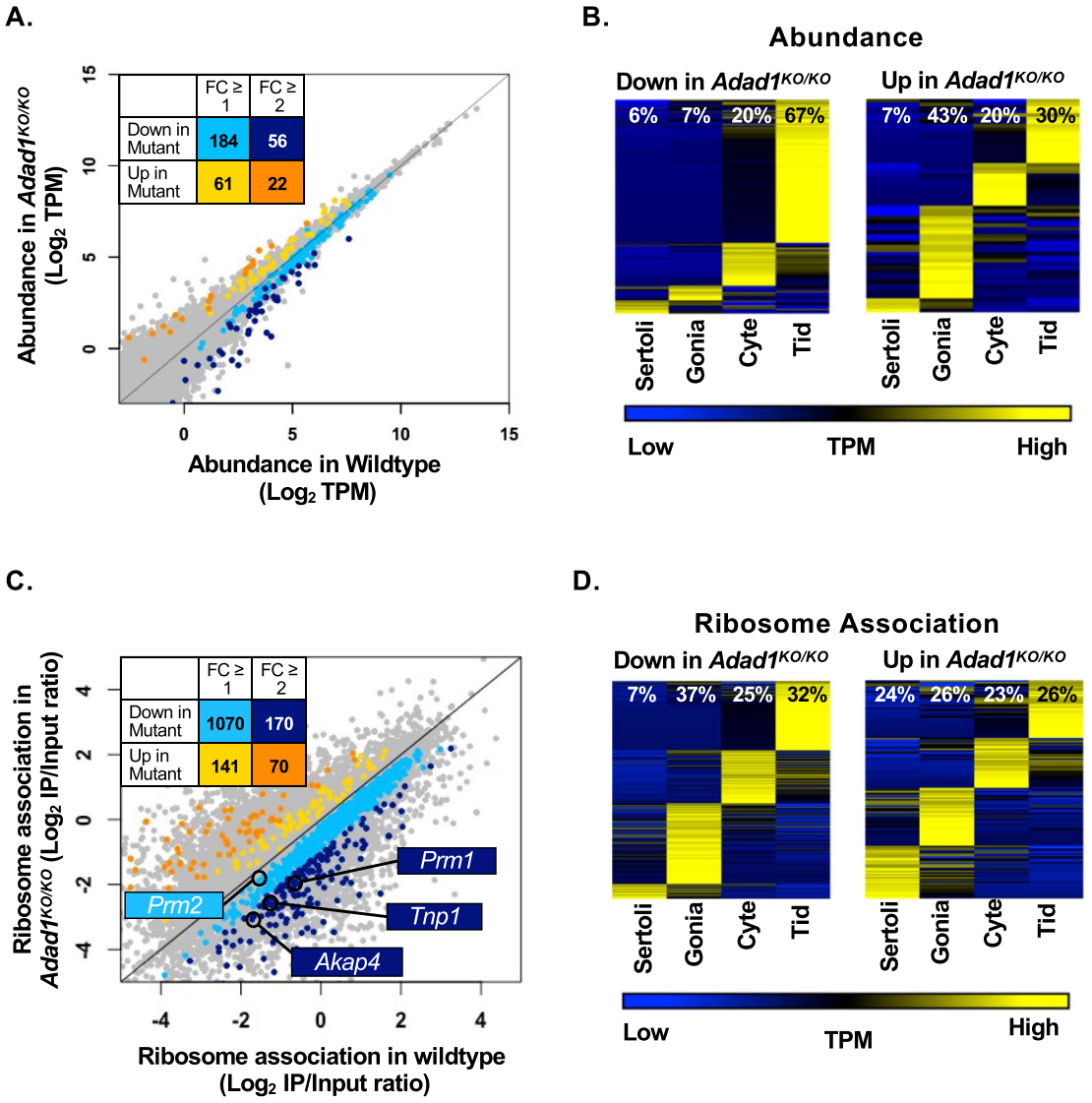

Figure 1. *Adad1* mutant testes display limited changes in transcript abundance but many transcripts with reduced ribosome association. (A) Total transcript abundance in 28 dpp wildtype and *Adad1*$^{KO/KO}$ demonstrates very few transcripts with significant differential expression (DE) in *Adad1* mutant testes. Orange and blue points—significantly DE ($P \leq 0.05$ by EBSeq differential expression analysis). Number of significant DE genes reported in table inset. (B) Expression of DE genes in isolated cells from wildtype testes demonstrates enrichment of spermatid expression in *Adad1*$^{KO/KO}$ downregulated genes. (C) Ribosome association (RA) of transcripts in 28 dpp wildtype and *Adad1*$^{KO/KO}$ demonstrates many transcripts have significantly reduced RA in *Adad1*$^{KO/KO}$ testis. Orange and blue points—significantly differentially ribosome associated (DRA) ($P \leq 0.05$ by Welch's *t*-test). Number of genes identified as significantly DRA reported in table inset. Select spermiogenesis genes of interest indicated, colors indicate DRA class defined in table inset. (D) Expression of DRA genes in isolated cells from wildtype testes demonstrates enrichment of numerous spermatid genes. Gonia—spermatogonia, Cyte—spermatocyte, Tid—spermatid. Percentage of DE or DRA genes with each cell type expression profile reported.

association in *Adad1* mutants. This suggests that ADAD1 may influence translation of key spermiogenesis genes, thus leading to the ADAD1 phenotype.

Reduced ribosome association is linked to delayed protein production

To further explore whether reduced ribosome association resulted in abnormal translation of proteins important for spermiogenesis, we defined the temporal appearance of two physiologically relevant transcripts, *Tnp1* and *Akap4*. Both had reduced ribosome association in the mutant and both have previously been identified as targets of translation regulation in post-meiotic germ cells [6, 43]. In addition, both are associated with processes that appear abnormal in *Adad1* mutant sperm. TNP1 is fundamental for normal genome compaction [14] and AKAP4 facilitates the signaling necessary for normal sperm motility [44].

Previous studies have successfully used a temporal approach to identify abnormal translation regulation in male germ cells [15]; however, this method relies heavily on accurate cell identification that requires tubule cross-section staging. Unfortunately, most staging techniques utilize morphological features of post-meiotic germ cells, which are perturbed in *Adad1* mutants. To resolve this, we developed a stage identification method using a combination of mitotic and meiotic germ cell morphologies along with the meiotic marker synaptonemal complex protein 3 (SYCP3)

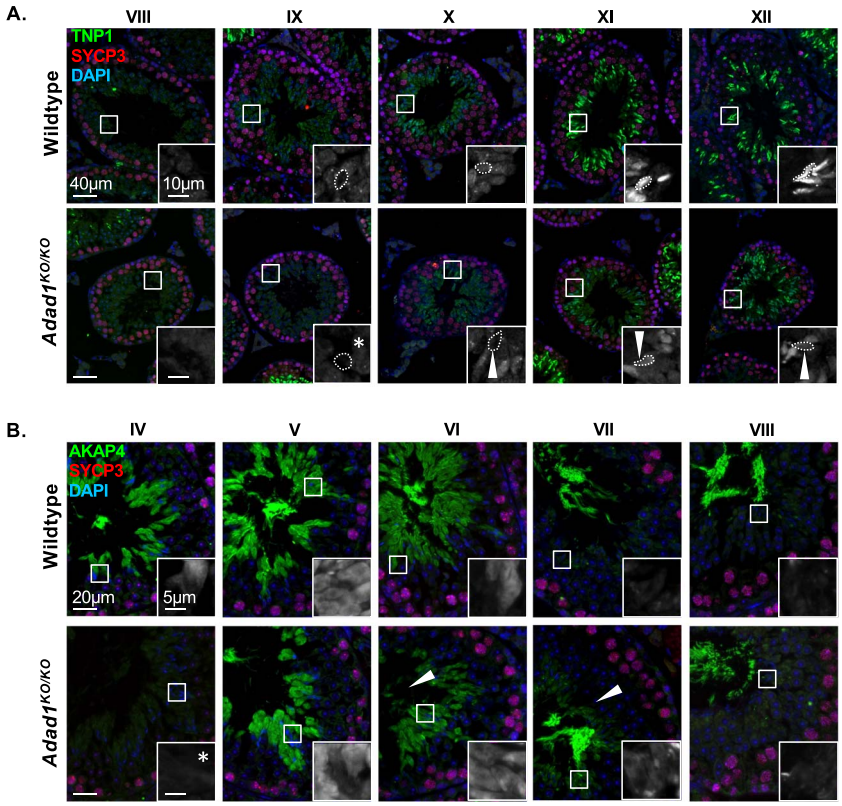

Figure 2. Translation and transport of proteins important to spermatogenesis are delayed or reduced in *Adad1* mutant spermatids. (A) Immunofluorescence of TNP1 in adult wildtype and *Adad1*$^{KO/KO}$ testis sections by stage showing delayed translation of TNP1 (asterisks) and failure to import into the nucleus (arrowheads) in mutants. Dashed line in insets—nucleus. (B) Immunofluorescence of AKAP4 in adult wildtype and *Adad1*$^{KO/KO}$ testis sections by stage showing delayed translation of AKAP4 (asterisks) and delayed tail import along with failure to export from the cytoplasm (arrowheads) in mutants. All images are representative of biological triplicate. Inset location indicated by box. Stage indicated by Roman numeral. For individual image staging criteria, see Supplementary Figure S7.

(Supplementary Figure S3). This approach allows highly accurate cross-section staging even in the case of abnormal post-meiotic germ cells, such as in *Adad1* mutants.

Using our newly developed staging technique, we examined TNP1 in wildtype and mutant adult testes (Figure 2A) by stage. Translation of *Tnp1* is temporally regulated, with transcript accumulating in round spermatids and undergoing translation suppression until translation is activated upon spermatid elongation [6]. Thus, early appearance of TNP1 protein is indicative of failed translation suppression while a delay indicates failed translation activation. Under normal circumstances, spermatids accumulate cytoplasmic TNP1 by step 9, as is observed in wildtype spermatids. However, in *Adad1* mutant testes, cytoplasmic TNP1 accumulation was not widespread until step 10. To confirm that this delay was not a function of overall cellular delay, we examined dissolution of the chromatoid body, a process uninfluenced by genome compaction or head shaping, by IF detection of the chromatoid body marker piwi-like protein 1 (PIWIL1) [45] (Supplementary Figure S4A). In wildtype spermatids, PIWIL1 remains localized to the chromatoid body until round spermatids mature into elongating spermatids at step 10. This localization pattern is clearly retained in mutant spermatids, demonstrating that *Adad1* mutation does not directly influence maturation of spermatids during the round-to-elongated transition. Based on this, the observed delay in *Tnp1* translation is likely a function of the molecular activity of ADAD1 itself.

A similar analysis was performed for AKAP4, which in wildtype spermatids first appears as a cytoplasmic protein in step 14 elongated spermatids of stage II/III [43] (Figure 2B). In contrast, *Adad1* mutant spermatids fail to initiate AKAP4 protein production until step 15 in stage IV. Quantification of the above phenomenon (Supplementary Figure S4B and C) confirmed a delay in both *Tnp1* and *Akap4* translation in *Adad1* mutants. For both *Tnp1* and *Akap4*, ribosome association was found to be significantly reduced while transcript abundance was effectively unchanged (Supplementary Figure S4D). This, along with delayed protein appearance of both TNP1 and AKAP4, demonstrates that ADAD1 is required for the normal translation of specific spermiogenesis-associated transcripts in elongating and elongated spermatids.

Adad1 mutant spermatids display distinct protein transport defects

Although significant, the above identified translation delay seems unlikely to result in the dramatic phenotypic changes observed in *Adad1* sperm. However, both proteins have distinct subcellular localizations that are required for their activity [14, 44], and previous reports have suggested abnormal translation may impact localization [15]. In wildtype testes, TNP1 is imported from the cytoplasm into the nucleus shortly after the protein is produced, in step 10 spermatids, a process that is complete by step 13 [46]. Nuclear TNP1 localization is required for DNA compaction via the histone–protamine exchange [47], which appears abnormal in *Adad1*

mutant sperm. A detailed examination of TNP1 localization in *Adad1* mutants showed substantial defects (Figure 2A and Supplementary Figure S4B). In addition to a delay in nuclear import, complete nuclear import was never achieved, with the majority of spermatids showing both cytoplasmic and nuclear signal throughout development. Thus, reduced nuclear TNP1 localization along with reduced translation may be partially causative to the abnormal DNA compaction of *Adad1* mutant sperm.

Like TNP1, AKAP4 has a distinct developmental protein localization wherein it is loaded onto the growing spermatid tail starting in stage II–III step 14 spermatids, nearly concurrent with the first appearance of protein [43] and is mostly complete by step 15 in stage V. Similar to TNP1, AKAP4 (Figure 2B and Supplementary Figure S4C) underwent delayed and reduced transport in *Adad1* mutant spermatids, as measured by clear AKAP4 cytoplasmic retention in a subset of spermatids through step 16 in stage VII. Functionally, once AKAP4 localizes to the sperm tail, it acts as structural protein of the fibrous sheath and facilitates anchoring of the PKA signaling complex, a process required for normal PKA activation and ultimately normal sperm motility [42]. Our previous observations suggested that PKA signaling was reduced in *Adad1* mutant sperm. Whether this was a direct effect of AKAP4 anchoring or a result of other signaling abnormalities, such as reduced cAMP response, remained unclear. However, treatment with the cAMP cascade agonist dibutyryl cAMP along with the phosphodiesterase inhibitor IBMX failed to rescue PKA signaling (Supplementary Figure S2C–F), mimicking what occurs when the AKAP–PKA interaction is inhibited via specific peptides such as Ht31 [48]. Together, these findings suggest that abnormal AKAP4 localization may be driving, at least in part, decreased PKA activity and sperm motility in *Adad1* mutants.

Neither TNP1 nor AKAP4 ever achieve completely normal localization; thus, these delays are unlikely to be exclusively due to delayed protein production. Supporting this notion, both have functions that rely on proper localization and those functions appear perturbed in *Adad1* mutants. Together, these results indicate that *Adad1* mutant spermatids not only have delayed translation but also show abnormal intracellular transport, leading to broad-scale defects in protein localization and function.

Loss of ADAD1 leads to distinct defects in the manchette, a spermatid-specific protein localization microtubule network

Given the distinct subcellular localization defects in *Adad1* mutant spermatids, we explored the possibility that intracellular transport was impacted by ADAD1 loss. The manchette, a multifunctional microtubule network that forms just prior to spermatid elongation, has been closely linked to intracellular transport along with sperm head shaping [49]. Likewise, known manchette mutants have distinct sperm morphologies that resemble *Adad1* mutant sperm [50–52], prompting us to examine manchette morphology in *Adad1* mutants. We first examined the localization of α-tubulin, a primary component of the manchette microtubule structure [53], in isolated spermatids from wildtype and mutant testes (Figure 3A). Staining in wildtype early elongating spermatids, which can be identified by an ovoid core of intense DAPI staining, showed a cup-shaped α-tubulin distribution. Late elongating wildtype spermatids, characterized by a narrow and pointed region of intense DAPI staining, were found to display the classic "grass skirt" structure indicative of a correctly formed manchette [50, 54]. In contrast, mutant early and late elongating spermatids showed dramatic defects in both the amount and distribution of α-tubulin. *Adad1* mutant manchette defects included abnormal polarization, localization, and α-tubulin abundance. Given the severity of the defects, we next asked how and when these abnormalities arose.

Timing of manchette formation and dissolution is abnormal in *Adad1* mutants

The above analysis relied on isolated cells, which do not provide the same developmental information as can be derived from analysis of intact testes. To define the developmental profile of manchette abnormalities in *Adad1* mutant spermatids, we stained wildtype and mutant testes for acetylated α-tubulin, which accumulates in the manchette [55] (Figure 3B). In wildtype spermatids, manchette-localized acetylated α-tubulin was first detected in step 9 spermatids wherein it formed distinct, polarized cup shapes along the basal aspect of the spermatid nucleus. Following this, signal gradually reduced until it was no longer observed in the spermatid cytoplasm, a process that is completed by step 11. While mutant spermatids also start to accumulate acetylated α-tubulin during step 9, acetylated α-tubulin localization showed a much more diffuse signal, especially in steps 10 through 12. In addition, manchette-associated acetylated α-tubulin was aberrantly retained in late elongated spermatids, not disappearing until step 15 in stage IV. These findings correlate well with the isolated cell analyses and strongly indicate abnormal manchette formation.

To determine if additional manchette-associated proteins showed any abnormal accumulation, localization, or dissolution, we next examined β-tubulin, another major component of the manchette [53] (Figure 3C). In both wildtype and *Adad1* mutant spermatids, β-tubulin begins to accumulate in the manchette in step 8 spermatids. However, while β-tubulin staining showed a classic manchette structure in wildtype spermatids, it displayed abnormal polarization and localization in *Adad1* mutant spermatids, mimicking the α-tubulin staining seen previously. Furthermore, β-tubulin association with the manchette in mutant spermatids was also retained beyond that observed in wildtype spermatids, with manchette signal disappearing by step 15 in stage V in wildtype but remaining until step 15 in stage VI in *Adad1* mutant spermatids. The obvious delay in manchette dissolution as well as the abnormal morphology as seen by α-tubulin, acetylated α-tubulin, and β-tubulin suggests that there is defective regulation of the manchette in *Adad1* mutant spermatids. It seems likely that this deregulation is the primary driver of abnormal sperm head shape and size in *Adad1* mutants.

Although previous analyses demonstrated minimal changes on the total transcript level, we wondered whether manchette transcripts may show abnormal ribosome association in *Adad1* mutants (Supplementary Figure S5). Of the 54 manchette-associated genes listed in [56], three (coiled-coiled domain containing 42 - *Ccdc42*, RIMS binding protein 3 - *Rimbp3*, and Sad1 and UNC84 domain containing 3 - *Sun3*) were found to have reduced ribosomal association in *Adad1* mutants while two (SNAP-associated protein - *Snapin* and

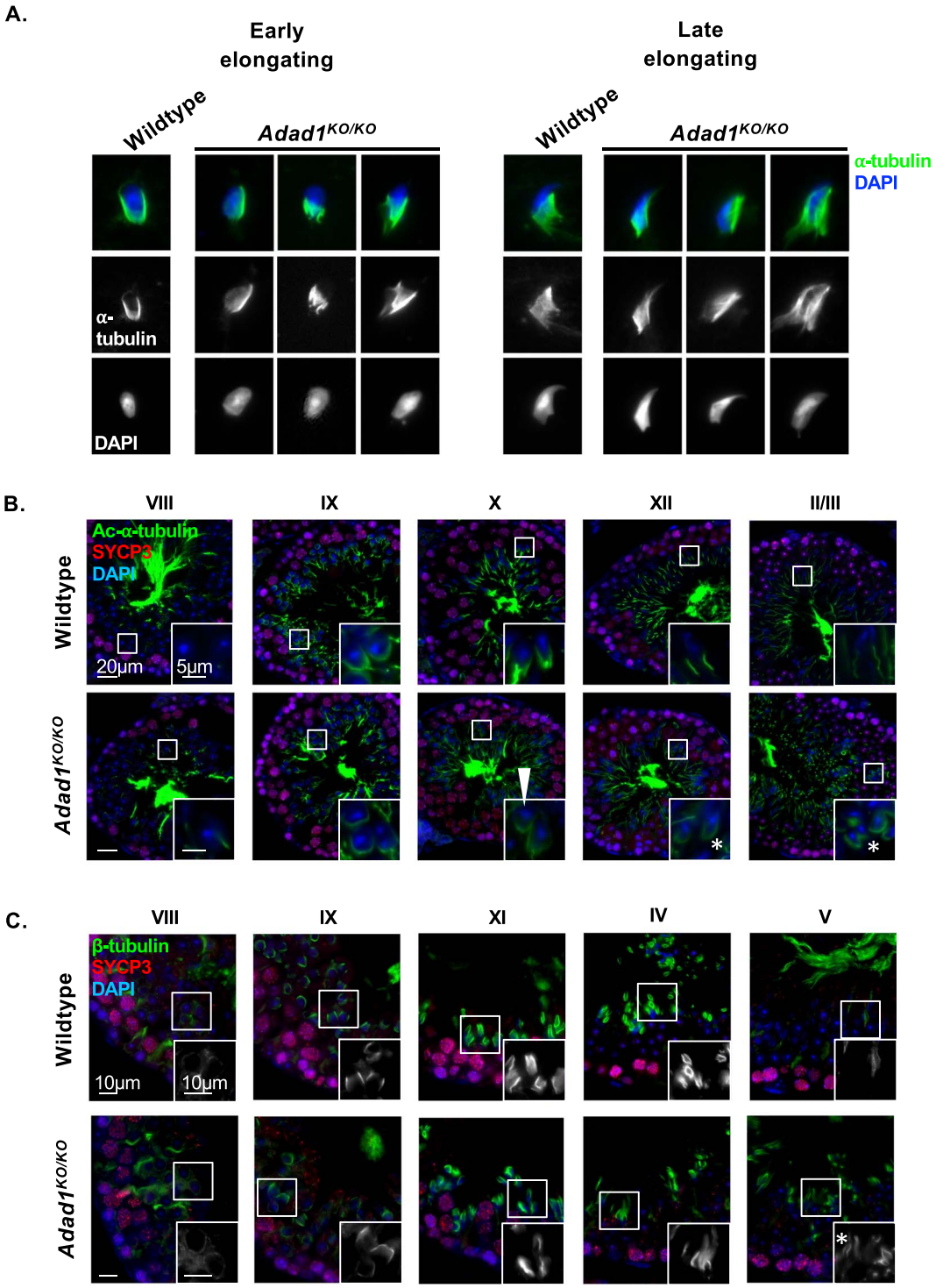

Figure 3. *Adad1* mutants have abnormal manchette morphology. (A) ICC of α-tubulin in adult wildtype and *Adad1*$^{KO/KO}$ testicular cell spreads shows abnormal localization in both early and late elongating spermatids. (B) Immunofluorescence of acetylated-α-tubulin (Ac-α) in adult wildtype and *Adad1*$^{KO/KO}$ testis cross-sections shows delayed dismantling of the manchette (asterisks) along with abnormal acetylated-α-tubulin polarization (arrowhead) in mutants. (C) Immunofluorescence of β-tubulin in adult wildtype and *Adad1*$^{KO/KO}$ testis sections by stage showing abnormal localization (insets) and delayed dissolution (asterisks) in mutants. All images are representative of biological triplicate. Inset location indicated by box. Stage indicated by Roman numeral. For individual image staging criteria, see Supplementary Figure S7.

Sun3) were significantly reduced on the transcript level. The role of CCDC42 in manchette dynamics is debatable [57] and SNAPIN's primary function is to facilitate vesicle transport along microtubules [58]. As such, neither are likely to be a primary driver of manchette abnormalities in the *Adad1* mutant. In addition, while RIMBP3 has been implicated as regulating manchette placement [52], it had only minimally reduced ribosome association in the mutant making its role in ADAD1-driven manchette defects unclear. *Sun3*, however, which was reduced in both ribosome association and on the transcript level, encodes a core component of the linker of the nucleoskeleton and cytoskeleton (LINC) complex, which

connects the manchette to the nuclear matrix [59]. Thus, its reduction suggests some perturbation in the LINC complex with *Adad1* mutation.

LINC complex formation is abnormal in *Adad1* mutants

The LINC complex is composed of SYNE (spectrin repeat containing nuclear envelope protein, also known as KASH and NESPRIN) and SUN proteins [59], which directly interact both with the cytoplasmic microtubule network as well as the intranuclear lamins (Figure 4A). Mutation of LINC complex components can lead to defective sperm head shape [60], though detailed mechanistic understanding of how is still somewhat undefined. Given the abnormal head shape in *Adad1* mutant sperm along with the reduced expression and ribosome association of *Sun3*, we next investigated the protein localization and expression of key LINC complex components by developmental stage. We first examined SUN3 (Figure 4B), which showed accumulation in both wildtype and *Adad1* mutant spermatids starting at step 8 round spermatids, though with reduced intensity in mutant versus wildtype consistent with the overall reduced transcript abundance and ribosome association. While SUN3 demonstrated polarized localization similar to wildtype in step 8 spermatids, by step 11 spermatids localization was severely perturbed in *Adad1* mutant spermatids with reduced polarization and incomplete association with the entirety of the spermatid basal aspect. This was coupled to clear reduction of protein in step 12 spermatids. The abnormal polarization and localization was retained throughout mutant spermatid development until SUN3's disassociation with the manchette, which occurred at step 15 in stage V in wildtype but not until step 15 in stage VI in *Adad1* mutants.

Having observed abnormal abundance and localization for SUN3, we next examined SYNE1 (Figure 4C), which connects SUN3 to the cytoplasmic microtubule network [59]. As expected, in wildtype spermatids SYNE1 was first detected in step 9 spermatids as an accumulation along the basal aspect of spermatid nuclei in a shape reminiscent of the manchette cup structure. Detection in *Adad1* mutant spermatids did not occur until step 10. Although *Syne1* was not identified as DRA in our ribosome association analysis, direct examination of the data (Supplementary Figure S6A) revealed a trend for reduced ribosome association in mutants in the absence of altered transcript abundance. This pattern, in conjunction with delayed protein appearance, suggests that ADAD1 also influences the translation of *Syne1*. In conjunction with delayed appearance in mutant spermatids, once detected SYNE1 failed to display the distinct polarized accumulation observed in wildtype spermatids. In addition, SYNE1 displayed a delay in disassociation with the manchette, which occurs by step 15 in stage V in wildtype testis but not until step 15 in stage VI in *Adad1* mutant testis. SYNE1's failed disassociation aligns temporally with both SUN3 as well as β-tubulin, suggesting that the defects in both manchette formation and dissolution in *Adad1* mutants are coupled to abnormal LINC complex remodeling in *Adad1* mutant spermatids.

Lamins function as the primary structural element of the nuclear membrane [61]. As such, they play diverse roles in nuclear biology, including mediating interactions with the cytoplasmic manchette via the LINC complex [62]. As a last measure of LINC complex formation and remodeling, we investigated Lamin B3 in both wildtype and *Adad1* mutant testes as a function of cell development using a pan Lamin B2/3 antibody (Figure 5A). Lamin B2 is not detected in murine spermatids [63]; however, B3 is specifically known to localize to the basal aspect of developing spermatids [64] and is a likely binding partner for spermatid expressed SUN proteins [62]. Protein accumulation of Lamin B3 initiated in step 7 spermatids in both wildtype and mutant testes, with no quantitative differences in membrane association and polarization in mutants relative to wildtype. As expected based on normal protein accumulation, *Lmnb2*, which encodes both Lamin B2 and B3, had unchanged abundance and ribosome association in the mutant (Supplementary Figure S6A). However, by step 9, there was a distinct localization failure in mutant spermatids. Furthermore, in step 10 wildtype spermatids Lamin B3 was no longer detected but was still highly abundant in *Adad1* mutant spermatids, mirroring localization and polarization abnormalities observed in β-tubulin, SYNE1, and SUN3. Quantification of this observation (Supplementary Figure S6B) confirmed the initial analyses. Together, these results demonstrate that lamin distribution, but not translation, in mutant spermatids is abnormal, which may be contributing to the observed changes in LINC complex formation and dissolution (Figure 5B). In addition, they suggest that elongating spermatid nuclear structure initiates properly in mutant spermatids but defects arise shortly thereafter.

Loss of ADAD1 leads to reduced translation of multiple nuclear pore complex components

While the defect in LINC complex remodeling may be causative to the *Adad1* phenotype, we wondered whether other nuclear dynamics may also be impacting germ cell development with ADAD1 loss. To that end, we focused on members of the nuclear pore complex (NPC). The NPC is a multifaceted regulator of nuclear biology, acting as the primary mechanism for nuclear import and export of proteins and mRNAs [65] while also defining nuclear structure via association with both the intranuclear lamina [66] and the cytoplasmic manchette [67].

To determine the impact of ADAD1 loss on the NPC, we queried our ribosome association and expression data for NPC components (Figure 6A). This analysis identified multiple transcripts encoding NPC proteins with reduced ribosome association in the mutant. Of special interest were nuclear pore membrane protein 121 (*Pom121*) and nucleoporin 210 (*Nup210*), which encode two of the three core NPC proteins [68]. These proteins span the nuclear membrane and their loss has profound impacts on the NPC as well as overall nuclear structure [69, 70]. Immunofluorescent localization of POM121 in elongating spermatids (Figure 6B) demonstrated a distinct polarized localization starting at step 9 and continuing through to step 12 in the wildtype. In the mutant, polarization as well as signal intensity was reduced at first detection, in step 9 spermatids. These abnormalities continued throughout spermatid development. Similarly, NUP210 (Figure 6C) appeared reduced with abnormal localization in mutant spermatids relative to wildtype. However, these defects arose somewhat later than for POM121, in step 12 spermatids. Together, the reduced ribosome association and reduced signal intensity of POM121 and NUP210 in mutant spermatids suggest that regulating translation of the NPC encoding transcripts is a primary function of ADAD1 and strongly imply the *Adad1* mutant phenotype is, at least in part, a result of abnormal NPC function and/or localization early in elongating spermatid development.

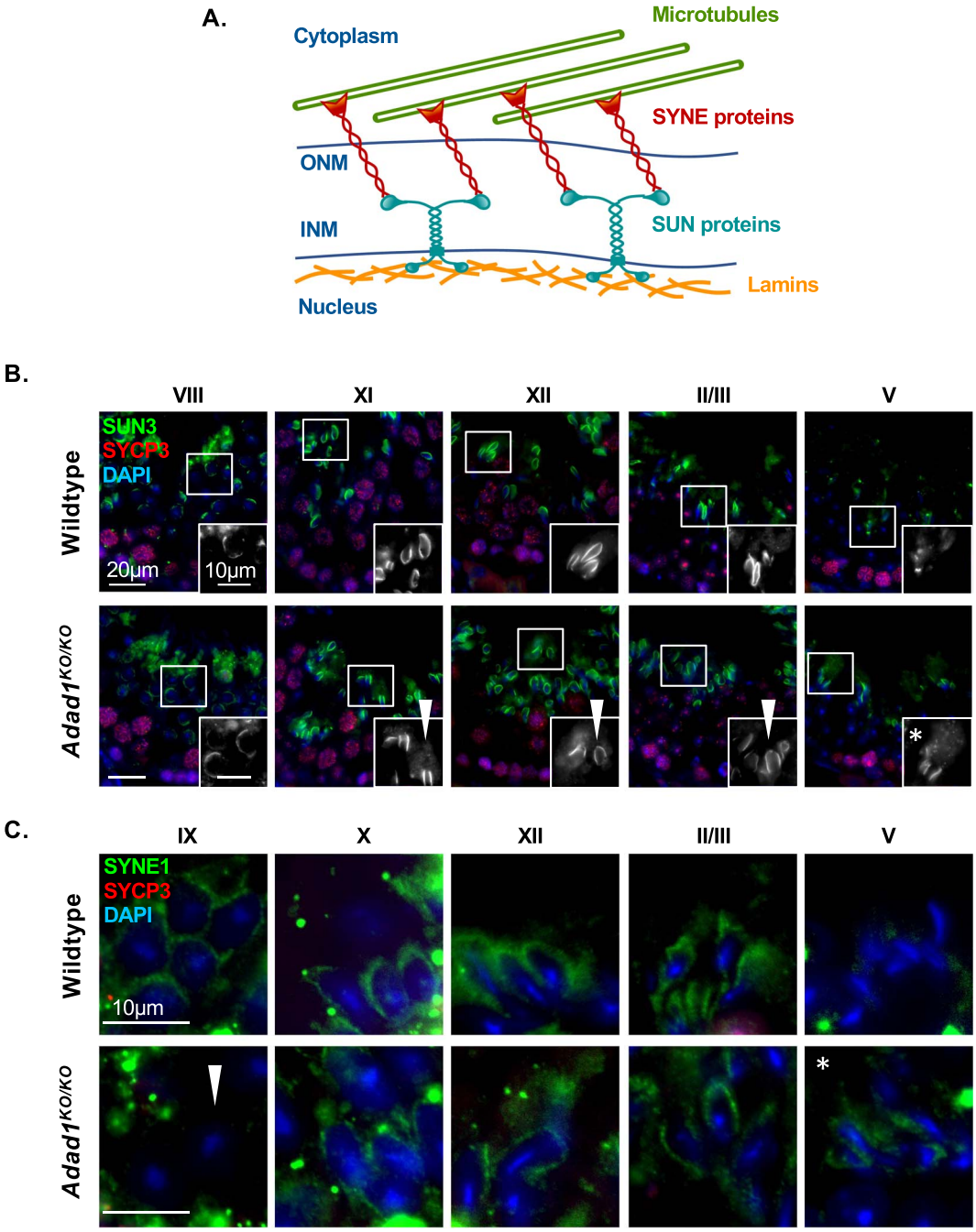

Figure 4. Loss of ADAD1 leads to abnormal LINC complex structure and dissolution. (A) Structural components of the LINC complex and how they interact with the microtubules of the manchette. ONM—outer nuclear membrane, INM—inner nuclear membrane. (B) Immunofluorescence of SUN3 in adult wildtype and *Adad1*$^{KO/KO}$ testis sections showing abnormal localization (arrowheads) and delayed dissolution (asterisks) in mutants. (C) Immunofluorescence of SYNE1 in adult wildtype and *Adad1*$^{KO/KO}$ testis sections showing delayed translation (arrowhead) and delayed dissolution (asterisk) in mutants. All images are representative of biological triplicate. Inset location indicated by box. Stage indicated by Roman numeral. For individual image staging criteria, see Supplementary Figure S7.

Discussion

The underlying drivers of the *Adad1* mutant phenotype have been, to date, unknown. This work represents the first attempt to define on a physiological and molecular level the role of ADAD1 during spermiogenesis. Our analyses show that loss of ADAD1 leads to reduced sperm motility along with distinct sperm head morphological defects, in particular reduced DNA compaction and overall head volume. A recent study suggests a similar impact of *ADAD1* mutation in humans as individuals with pathogenic *ADAD1* mutations present with reduced sperm motility and sperm head shape abnormalities [71]. Although *Adad1* mutant testes show minimal gene expression changes, the dramatic reduction of ribosome association in numerous spermatid transcripts demonstrates that ADAD1 influences translation of specific transcripts. This is further supported by delayed protein accumulation of two well-defined targets of translation regulation, *Tnp1* and *Akap4*, important for DNA compaction [14] and sperm tail

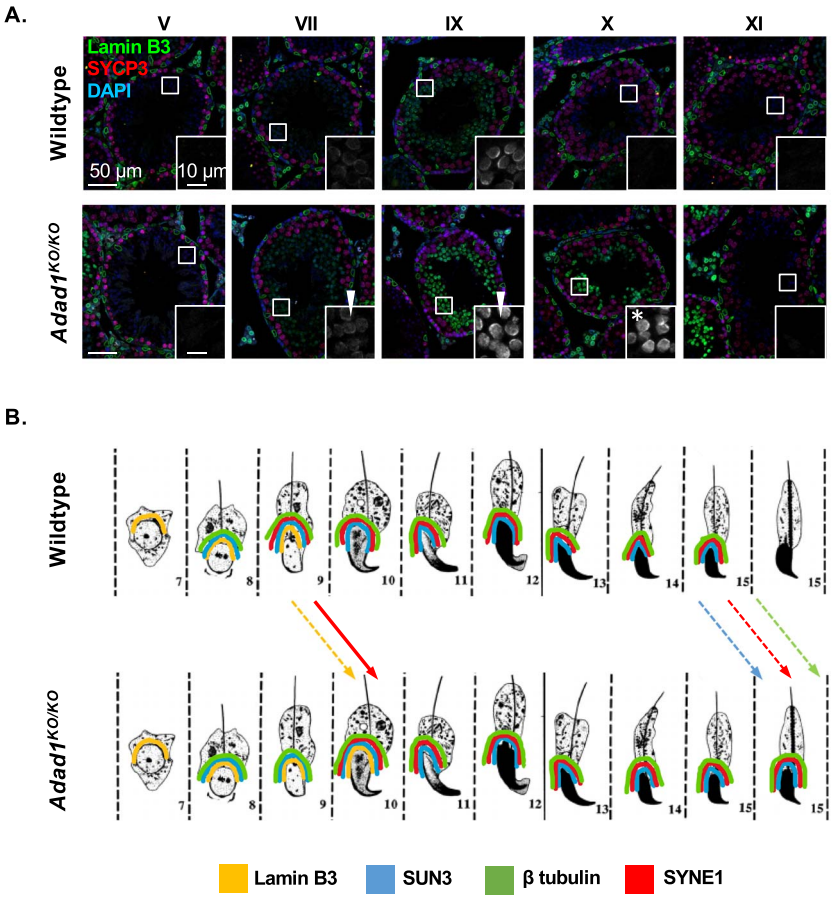

Figure 5. Loss of ADAD1 severely impacts nuclear lamin localization. (A) Immunofluorescence of Lamin B3 in adult wildtype and *Adad1*$^{KO/KO}$ testis sections showing abnormal polarization (arrowhead) and delayed dissolution (asterisk) in mutants. All images are representative of a biological triplicate. Inset location indicated by box. Stage indicated by Roman numeral. For individual image staging criteria, see Supplementary Figure S7. (B) Order of assembly and disassembly of manchette and LINC components in wildtype and *Adad1*$^{KO/KO}$ during spermatid development from step 7 to step 16. Dashed arrows—dissolution delays. Solid line arrow—accumulation delay. Spermatid images and step assignments adapted from [26].

function [44], respectively. This, in the absence of delayed cellular differentiation, strongly implies that ADAD1 acts as a transcript-specific translation activator. An unexpected outcome of these analyses was the observation that *Adad1* mutant spermatids also showed delays in protein subcellular localization not explained exclusively by delayed protein accumulation. Coincident with the observed protein transport abnormalities, we observed severe manchette defects along with aberrations in the deposition, structure, and dissolution of the nuclear-cytoplasmic connecting LINC complex. Further exploration of nuclear dynamics in *Adad1* mutant spermatids revealed distinct translation defects in nuclear pore complex encoding transcripts including reduced ribosome association along with reduced or delayed protein accumulation and abnormal localization. Together, this work defines ADAD1 as a transcript-specific translation regulator important for normal elongating spermatid nuclear dynamics and sperm morphogenesis.

The primary goal of this work was to identify the molecular function of ADAD1 during spermiogenesis. Previous works had proposed it to be involved in translation regulation and/or RNA editing [19, 21]. The second proposal was based on the presence of an adenosine deaminase (AD) domain in ADAD1 and the observation that many AD domain-containing proteins influence RNA editing [22]. However, more recent work demonstrated limited impact on mRNA editing in *Adad1* mutants [20], bringing the current understanding into question. The data reported here suggest that ADAD1 functions at the level of translation in the round spermatid. Although our analysis is unable to define cell-level changes in translation, the approach was designed to detect population-level changes, specifically in round spermatids. Reduced ribosome association coupled to delayed protein accumulation suggests ADAD1 is required for the normal accumulation of specific transcripts on the ribosome. While very few transcript-specific translation activators have been identified in the male germ cell, there is evidence in other systems that male germ-cell expressed RNA-binding proteins can act as such in specific contexts. For example, DAZL (deleted in azoospermia-like) acts as a translation activator in oocytes [72] while pumilio proteins have been shown to have non-canonical translation activating properties in embryonic stem cells [73].

Although the exact mechanism by which ADAD1 acts remains unclear, insight on a potential mechanism can be found from studies of other AD domain-containing proteins. Several recent reports have identified roles for AD domain-containing proteins in various aspects of RNA biogenesis, including splicing [74] and mRNA abundance [75]. Of special relevance to ADAD1, a widely expressed AD domain-containing protein, ADAR (adenosine deaminase,

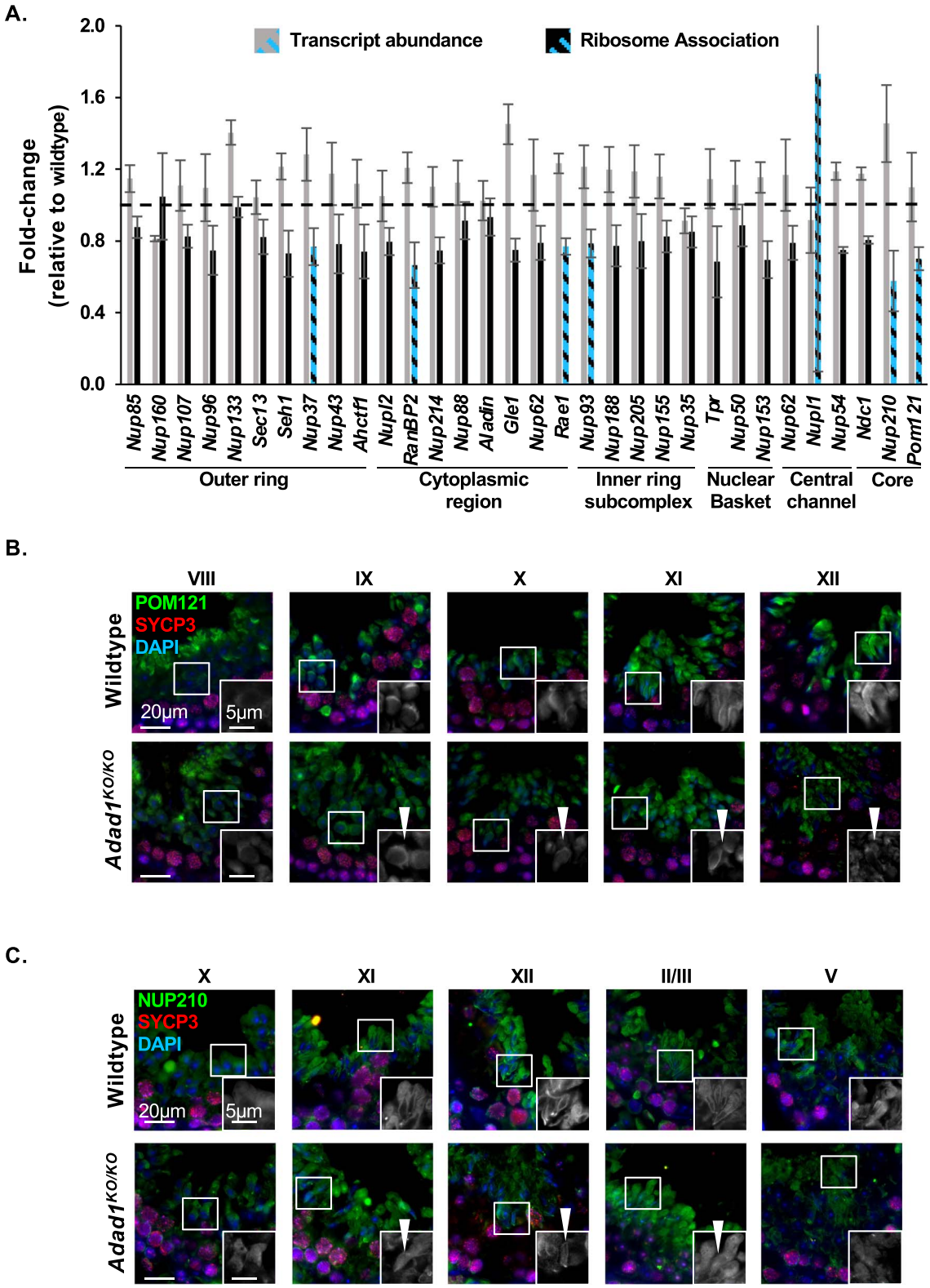

Figure 6. Loss of ADAD1 leads to reduced translation of multiple nuclear pore complex components. (A) Relative expression and ribosome association of NPC-associated genes [68] in *Adad1*$^{KO/KO}$ mutant testes. Nuclear pore region indicated below. Dashed line—wildtype average. Blue diagonal striped bars—significantly different from wildtype. $N = 3$/genotype. Error bars—SD. (B) Immunofluorescence of POM121 in adult wildtype and *Adad1*$^{KO/KO}$ testis sections showing abnormal localization of POM121 (arrowheads) and reduction in mutants. Inset location indicated by box. (C) Immunofluorescence of NUP210 in adult wildtype and *Adad1*$^{KO/KO}$ testis sections showing abnormal localization (arrowheads) and reduction in mutants. All images are representative of a biological triplicate. Inset location indicated by box. Stage indicated by Roman numeral. For individual image staging criteria, see Supplementary Figure S7.

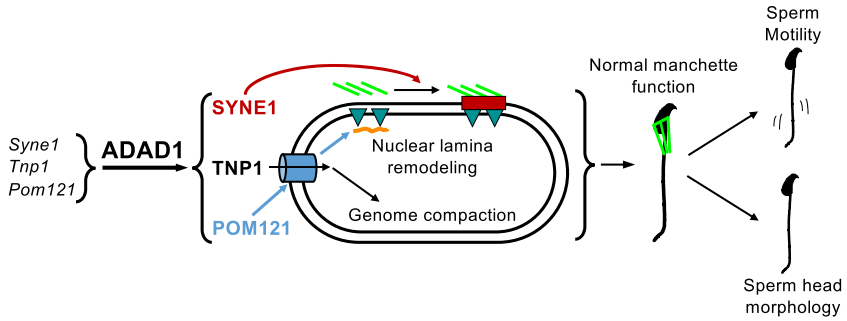

Figure 7. Proposed model of ADAD1 action. In elongating spermatids, ADAD1 regulates the translation of transcripts important for spermiogenesis, including those encoding the histone replacement protein TNP1 and proteins of the nuclear pore and LINC complexes. The correct translation of these transcripts leads to normal NPC (blue barrel) and LINC complex (bright green lines—microtubules, maroon box—SYNE proteins, teal triangles—SUN proteins, orange lines—nuclear lamins) formation early in spermiogenesis, thus facilitating normal genome compaction and nuclear lamina remodeling. These events then facilitate normal manchette formation and dissolution, in sum generating properly formed, motile sperm.

RNA-specific), modulates mRNA stability by competitively binding to double-stranded RNA structures in the 3′ UTR of mRNAs targeted for degradation [76]. This activity is mediated via its double-stranded RNA-binding motif (dsRBM), which is similar to the one found in ADAD1. While we observe no global transcript abundance changes in *Adad1* mutants, it is feasible that ADAD1 may influence transcript-specific translation by competitively inhibiting 3′ UTR binding by other regulatory RNA-binding proteins. Alternatively, ADAD1 may act indirectly to influence transcript-specific translation via an undefined mechanism. Future efforts will aim to address these outstanding mechanistic questions.

This work identified abnormalities in translation and/or localization in *Adad1* mutants of three intrinsically linked structures: the NPC, LINC complex, and manchette. In the context of the nuclear membrane, the NPC plays an especially important role in modulating both the protein composition and localization of the LINC complex and lamin matrix [77, 78]. Thus, it is unsurprising that in *Adad1* mutant spermatid defects in NPC composition are nearly concurrent with observed aberrations in nuclear lamins and other LINC complex components. However, it remains unclear whether LINC complex defects are exclusively due to NPC abnormalities, a direct effect of failed translation regulation by ADAD1, or a combination of both. Temporally, NPC and LINC complex alterations precede changes to the manchette, suggesting that they are upstream. Given this, we propose a model (Figure 7) whereby delayed and abnormal NPC and LINC remodeling in elongating spermatids lacking ADAD1 triggers a cascade of molecular events leading to abnormal manchette remodeling and protein localization. Ultimately, these aberrations give rise to the range of physiological deficiencies observed in mutant sperm. This work defines the NPC and LINC complex as targets of translational regulation in post-meiotic germ cells and ADAD1 as a key regulator thereof. Buoying our results, other reports have suggested that individual elements of the NPC are targets of regulated translation [79]. In total, these analyses define a new level of regulation for nuclear events in the spermatid and identify ADAD1 as a potent regulator via translation activation.

In addition to the above findings, this work describes several cases of transcripts with abnormal translation in *Adad1* mutant spermatids concurrent with failed intracellular protein transport of their products. Although translation timing and protein localization have been hypothesized to be coupled during spermiogenesis [15], no coherent mechanism has been described. A natural extension of our proposed model of ADAD1 action is that translation may be a key level of regulation for protein transport in the spermatid. This suggests that spermatids could leverage a cohesive process wherein the translation of functionally important proteins such as TNP1 and AKAP4 is coordinated with their transport via translation control of transport mechanisms such as the NPC and manchette. While over-simplified, this translation-transport model provides a platform from which new hypothesis can be generated and tested.

In addition to defining translation as a new level of regulation for the LINC complex, these studies represent the first time that formation dynamics for the manchette–LINC association has been described on this scale. Immunofluorescent studies of intact adult testes provide important development context missing in isolated cell analyses [80], the most common approach for manchette studies. By leveraging intact testes, our findings demonstrate the stepwise formation of the manchette–LINC connection, which appears to initiate with deposition of Lamin B3 along the nuclear membrane, followed by formation of the SUN3–lamin interaction, and finally connection to the microtubule network via SYNE1 that occurs concurrent to the loss of Lamin B3 in the nucleus. The interplay and interdependence of these steps are likely to be important drivers of post-meiotic germ-cell differentiation and as such represent important avenues for further study. Of particular interest is the observation that ADAD1 influences lamin deposition, likely as a result of its impact on the NPC and LINC complex. Lamins are known to be key drivers of chromosome dynamics during meiosis [81] and in particular play fundamental roles in chromosome bouquet formation, necessary for proper meiotic progression [82]. However, very little is known about whether lamins play a similar role in post-meiotic cells, which also display distinct telomeric localizations during spermiogenesis [83]. Identification of a homologous mechanism in post-meiotic cells would dramatically expand our understanding of chromosome dynamics as they relate to the fundamental process of spermatid genome organization.

In sum, our studies of *Adad1* mutant spermatids have revealed ADAD1 to be a transcript-specific translational activator during the later portion of spermiogenesis. In particular, it has profound impacts on two important nuclear complexes, the NPC and LINC complex, as well as an apparent

indirect effect on the manchette. Changes to these fundamental structures likely give rise to the myriad of cell physiology abnormalities in *Adad1* mutant spermatids. Furthermore, they suggest that translation regulation plays an important role in the proper temporal localization of post-meiotic germ-cell proteins. The outstanding questions stemming from this study regarding ADAD1 mechanism, protein transport regulation in spermatids, and spermatid NPC and LINC complex biology represent promising avenues that will shed considerable light on these relatively poorly studied aspects of male germ-cell biology.

Author Contributions

SP—methodology, validation, investigation, data curation, writing, visualization; CE—methodology, validation, investigation, data curation; AB—methodology, formal analysis, investigation, data curation; LC—methodology, investigation; TL—methodology, investigation; GM—methodology, investigation; PV—conceptualization, methodology, validation, formal analysis, resources, supervision; ES—conceptualization, methodology, validation, formal analysis, investigation, resources, data curation, writing, visualization, supervision, project administration, funding acquisition.

Supplementary Material

Supplementary Material is available at *BIOLRE* online.

Acknowledgment

The authors would like to thank current and previous members of the Snyder laboratory including Kelly Seltzer, Jeha Kim, and Megan Forrest for their support with animal husbandry, molecular analyses, and critical evaluation throughout the project.

Conflict of Interest: The authors have declared that no conflict of interest exists.

Data availability

All RNA-seq data for this manuscript are available at https://www.ncbi.nlm.nih.gov/sra under accession PRJNA907786. Remaining data are available from the corresponding author upon reasonable request.

References

1. Jan SZ, Hamer G, Repping S, de Rooij DG, van Pelt AMM, Vormer TL. Molecular control of rodent spermatogenesis. *Biochim Biophys Acta—Mol Basis Dis* 2012; **1822**:1838–1850.
2. Wei Y-L, Yang W-X. The acroframosome-acroplaxome-manchette axis may function in sperm head shaping and male fertility. *Gene* 2018; **660**:28–40.
3. Monesi V. Synthetic activities during spermatogenesis in the mouse. *Exp Cell Res* 1965; **39**:197–224.
4. Steger K. Transcriptional and translational regulation of gene expression in haploid spermatids. *Anat Embryol* 1999; **199**: 471–487.
5. Kleene KC, Distel RJ, Hecht NB. Translational regulation and deadenylation of a protamine mRNA during spermiogenesis in the mouse. *Dev Biol* 1984; **105**:71–79.
6. Steger K. Expression of mRNA and protein of nucleoproteins during human spermiogenesis. *Mol Hum Reprod* 1998; **4**:939–945.
7. Balhorn R, Weston S, Thomas C, Wyrobek AJ. DNA packaging in mouse spermatids. *Exp Cell Res* 1984; **150**:298–308.
8. Kleene KC. Patterns of translational regulation in the mammalian testis. *Mol Reprod Dev* 1996; **43**:268–281.
9. Lee K, Haugen HS, Clegg CH, Braun RE. Premature translation of protamine 1 mRNA causes precocious nuclear condensation and arrests spermatid differentiation in mice. *Proc Natl Acad Sci U S A* 1995; **92**:12451–12455.
10. Zhong J, Peters AHFM, Lee K, Braun RE. A double-stranded RNA binding protein required for activation of repressed messages in mammalian germ cells. *Nat Genet* 1999; **22**:171–174.
11. Braun RE. Packaging paternal chromosomes with protamine. *Nat Genet* 2001; **28**:10–12.
12. Balhorn R, Brewer L, Corzett M. DNA condensation by protamine and arginine-rich peptides: analysis of toroid stability using single DNA molecules. *Mol Reprod Dev* 2000; **56**:230–234.
13. Dogan S, Vargovic P, Oliveira R, Belser LE, Kaya A, Moura A, Sutovsky P, Parrish J, Topper E, Memili E. Sperm protamine-status correlates to the fertility of breeding bulls. *Biol Reprod* 2015; **92**: 1–9.
14. Yu YE, Zhang Y, Unni E, Shirley CR, Deng JM, Russell LD, Weil MM, Behringer RR, Meistrich ML. Abnormal spermatogenesis and reduced fertility in transition nuclear protein 1-deficient mice. *Proc Natl Acad Sci U S A* 2000; **97**:4683–4688.
15. Braun RE, Peschon JJ, Behringer RR, Brinster RL, Palmiter RD. Protamine 3′-untranslated sequences regulate temporal translational control and subcellular localization of growth hormone in spermatids of transgenic mice. *Genes Dev* 1989; **3**:793–802.
16. Hecht NB. Molecular mechanisms of male germ cell differentiation. *Bioessays* 1998; **20**:555–561.
17. Snyder E, Soundararajan R, Sharma M, Dearth A, Smith B, Braun RE. Compound heterozygosity for Y box proteins causes sterility due to loss of translational repression. *PLoS Genet* 2015; **11**:e1005690.
18. Yanagiya A, Delbes G, Svitkin YV, Robaire B, Sonenberg N. The poly(a)-binding protein partner Paip2a controls translation during late spermiogenesis in mice. *J Clin Invest* 2010; **120**:3389–3400.
19. Schumacher JM, Lee K, Edelhoff S, Braun RE. Distribution of Tenr, an RNA-binding protein, in a lattice-like network within the spermatid nucleus in the Mousel. n.d.; **10**:1274–1283.
20. Snyder E, Chukrallah L, Seltzer K, Goodwin L, Braun RE. ADAD1 and ADAD2, testis-specific adenosine deaminase domain-containing proteins, are required for male fertility. *Sci Rep* 2020; **10**:11536.
21. Connolly CM, Dearth AT, Braun RE. Disruption of murine Tenr results in teratospermia and male infertility. *Dev Biol* 2005; **278**: 13–21.
22. Nishikura K. A-to-I editing of coding and non-coding RNAs by ADARs. *Nat Rev Mol Cell Biol* 2016; **17**:83–96.
23. Sanz E, Yang L, Su T, Morris DR, McKnight GS, Amieux PS. Cell-type-specific isolation of ribosome-associated mRNA from complex tissues. *Proc Natl Acad Sci U S A* 2009; **106**: 13939–13944.
24. Chukrallah LG, Seltzer K, Snyder EM. RiboTag immunoprecipitation in the germ cells of the male mouse. *J Vis Exp* 2020;**157**:e60927.
25. Gaysinskaya V, Soh IY, van der Heijden GW, Bortvin A. Optimized flow cytometry isolation of murine spermatocytes. *Cytometry*, 2014;**85**:556–565. https://doi.org/10.1002/cyto.a.22463.
26. Russell LD, Ettlin RA, Sinha Hikim AP, Clegg ED. *Histological and Histopathological Evaluation of the Testis*, 1st ed. Clearwater, FL: Cache River Press; 1990.
27. Shima JE, McLean DJ, McCarrey JR, Griswold MD. The murine testicular transcriptome: characterizing gene expression in the testis during the progression of spermatogenesis. *Biol Reprod* 2004; **71**:319–330.
28. Ewels P, Magnusson M, Lundin S, Käller M. MultiQC: summarize analysis results for multiple tools and samples in a single report. *Bioinformatics* 2016; **32**:3047–3048.
29. Langmead B, Salzberg SL. Fast gapped-read alignment with bowtie 2. *Nat Methods* 2012; **9**:357–359.

30. Bolger AM, Lohse M, Usadel B. Trimmomatic: a flexible trimmer for Illumina sequence data. *Bioinformatics* 2014; **30**:2114–2120.
31. Marini F, Binder H. pcaExplorer: an R/Bioconductor package for interacting with RNA-seq principal components. *BMC Bioinformatics* 2019; **20**:331.
32. Gamble J, Chick J, Seltzer K, Graber JH, Gygi S, Braun RE, Snyder EM. An expanded mouse testis transcriptome and mass spectrometry defines novel proteins. *Reproduction* 2020; **159**:15–26.
33. Li B, Dewey CN. RSEM: accurate transcript quantification from RNA-Seq data with or without a reference genome. *BMC Bioinformatics* 2011; **12**:323.
34. Leng N, Dawson JA, Thomson JA, Ruotti V, Rissman AI, Smits BMG, Haag JD, Gould MN, Stewart RM, Kendziorski C. EBSeq: an empirical Bayes hierarchical model for inference in RNA-seq experiments. *Bioinformatics* 2013; **29**:1035–1043.
35. Carlucci M, Kriščiūnas A, Li H, Gibas P, Koncevičius K, Petronis A, Oh G. DiscoRhythm: an easy-to-use web application and R package for discovering rhythmicity. *Bioinformatics* 2020; **36**: 1952–1954.
36. Huang DW, Sherman BT, Lempicki RA. Systematic and integrative analysis of large gene lists using DAVID bioinformatics resources. *Nat Protoc* 2009; **4**:44–57.
37. Balhorn R. The protamine family of sperm nuclear proteins. *Genome Biol* 2007; **8**:227.
38. Mascetti G, Carrara S, Vergani L. Relationship between chromatin compactness and dye uptake for in situ chromatin stained with DAPI. *Cytometry* 2001; **44**:113–119.
39. Ferro A, Mestre T, Carneiro P, Sahumbaiev I, Seruca R, Sanches JM. Blue intensity matters for cell cycle profiling in fluorescence DAPI-stained images. *Lab Invest* 2017; **97**:615–625.
40. Bizzaro D, Manicardi GC, Bianchi PG, Bianchi U, Mariethoz E, Sakkas D. In-situ competition between protamine and fluorochromes for sperm DNA. *Mol Hum Reprod* 1998; **4**:127–132.
41. Lolis D, Georgiou I, Syrrou M, Zikopoulos K, Konstantelli M, Messinis I. Chromomycin A3-staining as an indicator of protamine deficiency and fertilization. *Int J Androl* 1996; **19**:23–27.
42. Freitas MJ, Vijayaraghavan S, Fardilha M. Signaling mechanisms in mammalian sperm motility. *Biol Reprod* 2017; **96**:2–12.
43. Chowdhury TA, Kleene KC. Identification of potential regulatory elements in the 5′ and 3′ UTRs of 12 translationally regulated mRNAs in mammalian spermatids by comparative genomics. *J Androl* 2012; **33**:244–256.
44. Miki K, Willis WD, Brown PR, Goulding EH, Fulcher KD, Eddy EM. Targeted disruption of the Akap4 gene causes defects in sperm flagellum and motility. *Dev Biol* 2002; **248**:331–342.
45. Meikar O, Vagin VV, Chalmel F, Sõstar K, Lardenois A, Hammell M, Jin Y, Ros MD, Wasik KA, Toppari J, Hannon GJ, Kotaja N. An atlas of chromatoid body components. *RNA* 2014; **20**:483–495.
46. Zhao M, Shirley CR, Mounsey S, Meistrich ML. Nucleoprotein transitions during spermiogenesis in mice with transition nuclear protein Tnp1 and Tnp2 mutations. *Biol Reprod* 2004; **71**: 1016–1025.
47. Shirley CR, Hayashi S, Mounsey S, Yanagimachi R, Meistrich ML. Abnormalities and reduced reproductive potential of sperm from Tnp1- and Tnp2-null double mutant mice. *Biol Reprod* 2004; **71**: 1220–1229.
48. Rahamim Ben-Navi L, Almog T, Yao Z, Seger R, Naor Z. A-kinase anchoring protein 4 (AKAP4) is an ERK1/2 substrate and a switch molecule between cAMP/PKA and PKC/ERK1/2 in human spermatozoa. *Sci Rep* 2016; **6**:37922.
49. Kierszenbaum AL. Intramanchette transport (IMT): managing the making of the spermatid head, centrosome, and tail. *Mol Reprod Dev* 2002; **63**:1–4.
50. Cole A, Meistrich ML, Cherry LM, Trostle-Weige PK. Nuclear and manchette development in spermatids of normal and azh/azh mutant mice. *Biol Reprod* 1988; **38**:385–401.
51. Liu Y, DeBoer K, de Kretser DM, O'Donnell L, O'Connor AE, Merriner DJ, Okuda H, Whittle B, Jans DA, Efthymiadis A, McLachlan RI, Ormandy CJ, *et al*. LRGUK-1 is required for basal body and manchette function during spermatogenesis and male fertility. *PLoS Genet* 2015; **11**:e1005090.
52. Zhou J, Du Y-R, Qin W-H, Hu Y-G, Huang Y-N, Bao L, Han D, Mansouri A, Xu G-L. RIM-BP3 is a manchette-associated protein essential for spermiogenesis. *Development* 2009; **136**:373–382.
53. Fawcett DW, Anderson WA, Phillips DM. Morphogenetic factors influencing the shape of the sperm head. *Dev Biol* 1971; **26**: 220–251.
54. Courtens JL, Loir M, Delaleu B, Durand J. The spermatid manchette of mammals : formation and relations with the nuclear envelope and the chromatin. *Reprod Nutr Dévelop* 1981; **21**: 467–477.
55. Mochida K, Tres LL, Kierszenbaum AL. Isolation of the rat spermatid manchette and its perinuclear ring. *Dev Biol* 1998; **200**: 46–56.
56. Teves M, Roldan E, Krapf D, Strauss J III, Bhagat V, Sapao P. Sperm differentiation: the role of trafficking of proteins. *IJMS* 2020; **21**:3702.
57. Tapia Contreras C, Hoyer-Fender S. CCDC42 localizes to manchette, HTCA and tail and interacts with ODF1 and ODF2 in the formation of the male germ cell cytoskeleton. *Front Cell Dev Biol* 2019;**11**:7.
58. Ilardi JM, Mochida S, Sheng Z-H. Snapin: a SNARE–associated protein implicated in synaptic transmission. *Nat Neurosci* 1999; **2**:119–124.
59. Kmonickova V, Frolikova M, Steger K, Komrskova K. The role of the LINC complex in sperm development and function. *IJMS* 2020; **21**:9058.
60. Gao Q, Khan R, Yu C, Alsheimer M, Jiang X, Ma H, Shi Q. The testis-specific LINC component SUN3 is essential for sperm head shaping during mouse spermiogenesis. *J Biol Chem* 2020; **295**: 6289–6298.
61. Dittmer TA, Misteli T. The Lamin protein family. *Genome Biol* 2011; **12**:222.
62. Göb E, Schmitt J, Benavente R, Alsheimer M. Mammalian sperm head formation involves different polarization of two novel LINC complexes. *PloS One* 2010; **5**:e12072.
63. Vester B, Smith A, Krohne G, Benavente R. Presence of a nuclear lamina in pachytene spermatocytes of the rat. *J Cell Sci* 1993; **104**: 557–563.
64. Schütz W, Alsheimer M, Öllinger R, Benavente R. Nuclear envelope remodeling during mouse spermiogenesis: postmeiotic expression and redistribution of germline Lamin B3. *Exp Cell Res* 2005; **307**:285–291.
65. Kabachinski G, Schwartz TU. The nuclear pore complex—structure and function at a glance. *J Cell Sci* 2015; **128**:423–429.
66. Hawryluk-Gara LA, Shibuya EK, Wozniak RW. Vertebrate Nup53 interacts with the nuclear lamina and is required for the assembly of a Nup93-containing complex. *Mol Biol Cell* 2005; **16**: 2382–2394.
67. Lai T-H, Wu Y-Y, Wang Y-Y, Chen M-F, Wang P, Chen T-M, Wu Y-N, Chiang H-S, Kuo P-L, Lin Y-H. SEPT12-NDC1 complexes are required for mammalian spermiogenesis. *Int J Mol Sci* 2016; **17**:1911.
68. Khan AU, Qu R, Ouyang J, Dai J. Role of nucleoporins and transport receptors in cell differentiation. *Front Physiol* 2020; **11**.
69. Antonin W, Franz C, Haselmann U, Antony C, Mattaj IW. The integral membrane nucleoporin pom121 functionally links nuclear pore complex assembly and nuclear envelope formation. *Mol Cell* 2005; **17**:83–92.
70. Cohen M, Feinstein N, Wilson KL, Gruenbaum Y. Nuclear pore protein gp210 is essential for viability in HeLa cells and Caenorhabditis elegans. *Mol Biol Cell* 2003; **14**: 4230–4237.
71. Dai S, Liu M, Liu M, Jiang C, Yang Y, Han H, Yang Y, Jiang X, Shen Y. Population-based genetic analysis in infertile men reveals novel mutations of ADAD family members in patients with impaired spermatogenesis. *Hum Mol Genet* 2023;**32**:ddad012.

72. Yang C-R, Rajkovic G, Daldello EM, Luong XG, Chen J, Conti M. The RNA-binding protein DAZL functions as repressor and activator of mRNA translation during oocyte maturation. *Nat Commun* 2020; **11**:1–16.
73. Uyhazi KE, Yang Y, Liu N, Qi H, Huang XA, Mak W, Weatherbee SD, de Prisco N, Gennarino VA, Song X, Lin H. Pumilio proteins utilize distinct regulatory mechanisms to achieve complementary functions required for pluripotency and embryogenesis. *Proc Natl Acad Sci U S A* 2020; **117**:7851–7862.
74. Solomon O, Oren S, Safran M, Deshet-Unger N, Akiva P, Jacob-Hirsch J, Cesarkas K, Kabesa R, Amariglio N, Unger R, Rechavi G, Eyal E. Global regulation of alternative splicing by adenosine deaminase acting on RNA (ADAR). *RNA* 2013; **19**: 591–604.
75. Ganem NS, Ben-Asher N, Manning AC, Deffit SN, Washburn MC, Wheeler EC, Yeo GW, Zgayer OB-N, Mantsur E, Hundley HA, Lamm AT. Disruption in A-to-I editing levels affects C. elegans development more than a complete lack of editing. *Cell Rep* 2019; **27**:1244–1253.e4.
76. Sakurai M, Shiromoto Y, Ota H, Song C, Kossenkov AV, Wickramasinghe J, Showe LC, Skordalakes E, Tang H-Y, Speicher DW, Nishikura K. ADAR1 controls apoptosis of stressed cells by inhibiting Staufen1-mediated mRNA decay. *Nat Struct Mol Biol* 2017; **24**:534–543.
77. Jahed Z, Soheilypour M, Peyro M, Mofrad MRK. The LINC and NPC relationship—it's complicated! *J Cell Sci* 2016; **129**: 3219–3229.
78. Fiserova J, Goldberg MW. Relationships at the nuclear envelope: lamins and nuclear pore complexes in animals and plants. *Biochem Soc Trans* 2010; **38**:829–831.
79. Lautier O, Penzo A, Rouvière JO, Chevreux G, Collet L, Loïodice I, Taddei A, Devaux F, Collart MA, Palancade B. Co-translational assembly and localized translation of nucleoporins in nuclear pore complex biogenesis. *Mol Cell* 2021; **81**:2417–2427.e5.
80. Meistrich ML, Hess RA. Assessment of spermatogenesis through staging of seminiferous tubules. In: Carrell DT, Aston KI (eds.), *Spermatogenesis: Methods and Protocols*. Totowa, NJ: Humana Press; 2013: 299–307.
81. Wilson KL, Foisner R. Lamin-binding proteins. *Cold Spring Harb Perspect Biol* 2010; **2**:a000554.
82. Link J, Jahn D, Schmitt J, Göb E, Baar J, Ortega S, Benavente R, Alsheimer M. The meiotic nuclear lamina regulates chromosome dynamics and promotes efficient homologous recombination in the mouse. *PLoS Genet* 2013; **9**:e1003261.
83. Meyer-Ficca M, Muller-Navia J, Scherthan H. Clustering of pericentromeres initiates in step 9 of spermiogenesis of the rat (Rattus norvegicus) and contributes to a well defined genome architecture in the sperm nucleus. *J Cell Sci* 1998; **111**:1363–1370.